



# Estimates of Curie point depth, geothermal gradient and near-surface heat flow of Bida and environs, Nupe Basin, Nigeria, from high-resolution aeromagnetic data

M. O. Ole<sup>1</sup> · A. I. Opara<sup>1</sup> · C. N. Okereke<sup>1</sup> · C. P. Onyenegecha<sup>2</sup> · C. Z. Akaolisa<sup>1</sup> · A. E. Okoli<sup>1</sup> · O. J. Umoh<sup>1</sup>

Received: 17 September 2020 / Accepted: 8 December 2020 / Published online: 12 January 2021  
© Islamic Azad University (IAU) 2021

## Abstract

The Nupe Basin is a northwest–southeast (NW–SE) trending intracratonic sedimentary basin in the central part of Nigeria with its coordinates defined by longitude 5°00' to 8°00' E and latitude 7° 00' to 11° 00' N. Spectral inversion of the high-resolution aeromagnetic data was carried out to estimate the Curie point depth (CPD), geothermal gradient and heat flow regime of parts of the Nupe Basin, Nigeria. The estimate of regional temperature distribution and the identification of thermally active regions within the study area were made from the spectral analysis of high-resolution aeromagnetic data which were divided into 16 overlapping spectral blocks to obtain the top and centroid depths of the magnetic sources which were later used to calculate the heat flow characteristics. The estimated Curie point depths range from 21.43–26.71 km with an average CPD value of 24.54 km, while the geothermal gradient ranges between 21.72 °C km<sup>-1</sup> and 27.07 °C km<sup>-1</sup> with an average value of 24.39 °C km<sup>-1</sup>. Similarly, the estimated heat flow regime of the study area ranges from 54.30 m Wm<sup>-2</sup> to 67.67 m Wm<sup>-2</sup> with an average value of 59.41 m Wm<sup>-2</sup>. The range of estimated geothermal parameters in the study area is an indication that the area is not a volcanic or thermally active region and therefore has little potentials for geothermal energy exploitation. The geothermal play of the area, therefore, was revealed to be of the conduction-dominated play type, typically a combination of the basement and intracratonic basin geothermal play types.

**Keywords** Aeromagnetic · Basement depth · Geothermal energy · Curie point depth · Heat flow · Spectral inversion

## Introduction

Geothermal energy is the subsurface heat energy generated and stored within the earth, with the heat flow regime maintained by the various heat processes, including geodynamical, thermodynamical and radioactive decay processes within the earth's interior (Heicken 1982; Moeck 2014; Soltani et al. 2019). The need for clean, low-carbon, renewable energy resources targeted at the gradual but steady reduction of the carbon footprint that will facilitate the mitigation of the effects of climate change has led to increased interest in the exploration and exploitation of geothermal reservoirs

worldwide (IPCC 1990, 2014). Though significant growth in electricity generation from geothermal energy has been achieved worldwide in the last few decades, the high risk and cost of exploratory drilling to confirm the existence of viable geothermal resources remain the key challenges facing the industry (Bertani 2010). Also, the understanding and characterization of the geological controls of geothermal plays/reservoirs has been the topic of several recent studies (Heicken 1982; Moeck 2014; Soltani et al. 2019). These studies have most often focused on different scales ranging from plate tectonics (Muffler 1976; Heicken 1982), to local tectonics/structural geology including basement kinematics (Faulds et al. 2010; Opara et al. 2018), to the study of well logs and cores from the drilling of geothermal wells (Leary et al. 2013). A geothermal reservoir denotes the hot and permeable part of a geothermal system that may be directly exploited while a geothermal play is a conceptual model of key geological factors that affects the generation of recoverable geothermal resource at a specific structural position within a defined geologic setting (Moeck 2014).

✉ M. O. Ole  
olemosesonuegbe@gmail.com

<sup>1</sup> Department of Geology, School of Physical Sciences,  
Federal University of Technology Owerri, Owerri, Nigeria

<sup>2</sup> Department of Physics, School of Physical Sciences, Federal  
University of Technology Owerri, Owerri, Nigeria

Nigeria is a third world country battling with grossly insufficient power generation to satisfy its over 180 million people. This huge energy deficit has necessitated the exploration of alternative sources of clean and renewable energy resources including solar energy, wind, biofuels, geothermal, etc. Geothermal reservoirs and plays in Nigeria, in general, are mainly of the conduction-dominated play type: typically the basement and intracratonic basin geothermal play types which are found at deeper intervals of the crust than the convection-dominated types. The intracratonic basin geothermal plays, therefore, incorporate a reservoir within a sedimentary sequence laid down in an extensional graben or thermal sag basin (Heicken 1982; Moeck 2014). The long geological history of an intracratonic basin like the Nupe Basin usually produces sediment fill several kilometers thick that spans a wide range of depositional environments. Therefore, the exploration of the country's geothermal energy resources as an alternative power generation source has been prioritized by the government since the current hydropower generation from the Kanji Dam has not in any way met the required energy capacity and demands of her citizens. Though, geothermal energy as a major source of power has been known for several decades despite not being fully appreciated, explored, and exploited by most third world countries (Lawal et al. 2018). Despite this limitation, Ewa and Kryrowska (2010) posited that the exploration and exploitation of geothermal energy using geoscientific techniques is indeed very viable and possible.

Thermal properties of rocks (both brittle and ductile) determine the depths and degree of deformation of such rocks within the crust. Surficial estimates of these depths may be made from the rock's Curie point depth (CPD) and the thermal structure through the analysis of aeromagnetic data without necessarily carrying out in situ measurements within the region (Okubo et al. 1989; Tanaka et al. 1999). The Curie point depth (CPD) is the depth at which spontaneous magnetic dominant minerals lose their magnetization and transit from having ferromagnetic properties to the paramagnetic state as a result of increased temperatures beyond the critical point known as Curie temperature (Nagata 1961; Khojamli et al. 2016). Therefore, Curie temperature is usually estimated to be an approximate temperature of 580 °C at standard atmospheric pressure for magnetite-rich minerals (Khojamli et al. 2016). Tanaka et al. (1999) and Salk et al. (2005) postulated that there is usually a great spatial variation of CPD values due to contrast in geologic complexities and settings. Tanaka et al. (1999) compiled CPD estimates from several regions of the world and concluded that shallower CPD values of less than 10 km are usually associated with geodynamic environments and areas susceptible to tectonism and volcanic activities, whereas areas with CPD values between 15 km and 25 km are associated with ridges and island

arcs. Similarly, other areas with deeper CPD values of more than 25 km are generally associated with plateaus and trenches. A lot of works have been done to determine the CPD and thermal structure of various tectonic settings within the crust, both globally and within various basins in Nigeria, using high-resolution aeromagnetic data. Several documented studies on the application of geophysical methods in subsurface heat flow studies include the works on the relationship between heat flow processes and tectonics using magnetic and seismic data (Smith et al. 1974, 1977; Blakely 1988; Banerjee et al. 1998; Badalyan 2000), determination of CPD using statistical/fractal analyses of magnetic sources (Vacquier and Affleck 1941; Bhattacharyya and Leu 1975; Bansal et al. 2011; Abraham et al. 2018; Lawal & Nwankwo 2017), estimates of CPD, geothermal gradient and heat flow from aerogeophysical data (Byerly and Stolt 1977; Feumoe and Ndougsa-Mbarga 2017; Nwankwo and Sunday 2017; Lawal et al. 2018), and the application of CPD, geothermal gradient and heat flow in the study of thermal structure and geothermal energy exploration (Shuey et al. 1977; Blakely and Hassanza-deh 1981; Connard et al. 1983; Okubo et al. 1985; 1989; Okubo and Matsunaga 1994; Hisarli 1996; Tanaka et al. 1999; Dolmaz et al. 2005; Khojamli et al. 2016; Bello et al. 2017).

Curie point depth estimation based on spectral analysis of magnetic data has widely been used in the estimation of regional thermal structures (Bhattacharyya and Leu 1975; Spector and Grant 1970). At Curie temperatures, a magnetic substance loses its magnetic polarization. Consequently, it may be possible to locate a point on the isothermal surface by determining the depth to the bottom of a polarized rock mass (Byerly and Stolt 1977). Curie point depth is therefore the depth at which a rock mass loses its ferromagnetic properties due to increases in the temperature above the Curie temperature, which is approximately 580 °C. It is the depth at which a magnetic material passes from a ferromagnetic state to a paramagnetic state under the effect of increasing temperature (Abraham et al. 2015; Kasidi and Nur 2013; Tanaka et al. 1999). Though the concept of Curie point temperature may be controversial, Curie point depth (CPD) has been described by many authors (Kasidi and Nur 2012, 2013; Nwankwo et al. 2011; Stampolidis and Tsokas 2002; Stampolidis et al. 2005; Bertani 2010; Tanaka et al. 1999; Okubo et al. 1985; Bhattacharyya and Leu 1975). CPD has been applied over the years in the estimation of thermal structure in various regions and is often classified into two categories: (a) the determination and examination of the shape of the isolated magnetic anomalies (Bhattacharyya and Leu 1975) and (b) analysis of the statistical properties of the patterns of the magnetic anomalies (Spector and Grant 1970). The first method provides the relationship between the spectral characteristics of magnetic anomalies and the

depth of the magnetic source by carrying out a Fourier synthesis of the spatial data. The latter method is believed to be more appropriate in the compilation of the depth to the magnetic anomalies (Kasidi and Nur 2013; Shuey et al. 1977).

Spectral inversion techniques have been very effective in estimating the depths of magnetic sources because their operations are usually carried out in the frequency domain (Spector and Grant 1970). The technique has revealed that when a statistical population of a potential field source exists at a specific source depth, the expression of those sources on a plot of the natural logarithm of energy against wavenumber is a straight line having a slope of  $-4\pi h$  (Spector and Grant 1970). In heat flow estimation from aeromagnetic data, spectral inversion is usually on the residual data to infer the top depths of magnetic sources ( $Z_t$ ), and the centroid depths of the magnetic source ( $Z_o$ ) for the estimation of Curie point depths (CPDs). Several approaches have been used by several authors to calculate the depths to anomalous magnetic sources and centroid depths using the spectral inversion of high-resolution aeromagnetic (HRAM) data (Abd-El-Nabi 2012; Sayed et al. 2013; Abraham et al. 2014, 2015; Obande et al. 2014; Saleh et al. 2013; Lawal and Nwankwo 2017). Using the spectral inversion technique, the CPD is symbolically represented as  $Z_b$ , which is the depth to the bottom of magnetic sources (DBMS). It is described as such because, at such depth, the dominant magnetic minerals in the crust pass from the ferromagnetic state to a paramagnetic state under the influence of increasing temperatures (Hsieh et al. 2014). The centroid depths are the geometric centers (Okubo et al. 1985) of the vertical rectangular prismatic bodies (Spector and Grant 1970). Bhattacharyya (1966) used an expression for the power spectrum of the total magnetic field intensity over a single rectangular block, which was generalized by Spector and Grant (1970) by assuming that the anomalies on an aeromagnetic map are due to an ensemble of vertical prisms. Bhattacharyya and Leu (1975) and Okubo et al. (1985) also described  $Z_b$  as the basal depth of the magnetic sources which is assumed to be the CPD of the area hosting the magnetic sources. Several techniques, therefore, exist for the estimation of Curie point depths (Okubo et al. 1989; Bansal et al. 2013; Tanaka et al. 1999). Spector and Grant (1970) examined the pattern of the anomalies and provided the relationship between the spectrum of the magnetic anomalies and the depth of a magnetic source by carrying out a Fourier transform of the spatial data into the frequency domain. Okubo et al. (1989) summarized the methods of estimating the depth extent of magnetic sources and further categorized the different techniques into two groups: the group that examines the shapes of isolated magnetic anomalies (Bhattacharyya and Leu 1975) and the group that examines statistical properties of the patterns of the magnetic anomalies (Spector and Grant 1970). Both groups provide the relationship between the spectrum of magnetic

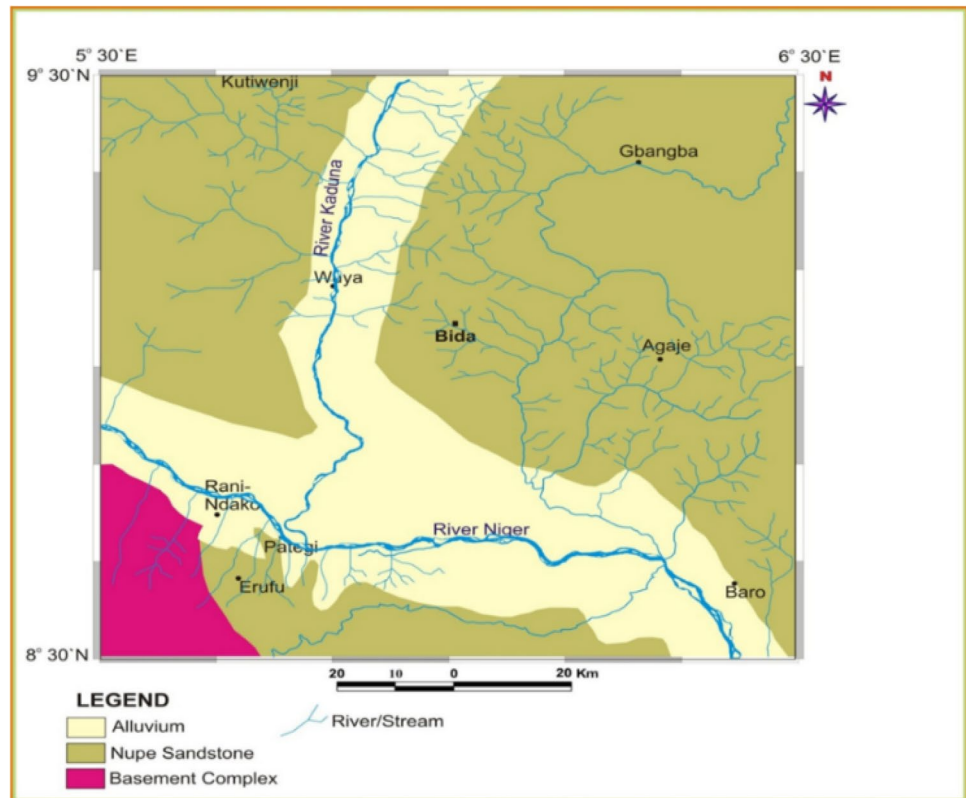
anomalies and the depth of the magnetic source by transforming the spatial data in the time domain to the frequency domain through Fourier transform processes.

The high-resolution airborne magnetic data used in this study are composed of four (4) high-resolution aeromagnetic maps of the Nigeria Geologic Survey Agency (NGSA), namely Bida, Agbaje, Pategi, and Baro with sheet numbers 183, 184, 204, and 205, respectively. This study was carried out between January to April 2020 with the main objective of estimating the Curie point depth (CPD), geothermal gradient and heat flow through the spectral inversion of high-resolution aeromagnetic data. The results of the present study will therefore help to evaluate the geothermal potentials of the study area.

### Location and geology of the study area

The study area is located between latitudes  $8^{\circ} 00' \text{ N}$ – $9^{\circ} 00' \text{ N}$  and longitudes  $6^{\circ} 30' \text{ E}$ – $7^{\circ} 30' \text{ E}$  and constitutes part of the southern Mid-Niger Basin also known as the Nupe Basin. The Nupe Basin is an NW–SE trending intracratonic sedimentary basin extending from Kontagora within the basement complex of Northern Nigeria to Lokoja and environs within the cretaceous sediments of the south (Adeleye 1974, Obaje 2009; Obaje et al. 2011, b). The Bida Basin, also known as the Mid-Niger or Nupe Basin located in north-central Nigeria, is one of the Cretaceous basins in West Africa whose origin is associated with the opening of the South Atlantic (Adeleye 1974; Obaje 2009; Obaje et al. 2011a, b). The study area is surrounded by the Precambrian basement rocks which experienced intense tectonism during the Late Pan-African phase ( $600 \pm 150 \text{ m.y.}$ ). These Pan-African episodes resulted in the development of shear zones that were subsequently reactivated during the Late Campanian–Maastrichtian resulting in wrench faulting which later formed the basin (Braide 1990; Obaje 2011, b). Ladipo 1988 suggested that the Nupe Basin is a gently down-warped trough whose origin is closely connected with the Santonian orogenic movement in southeastern Nigeria and the Benue valley, with its sedimentary fill comprising of post-orogeny molasses and thin, unfolded marine sediments. The Nupe Basin has an average sedimentary thickness of 3.5 km thick (Braide 1990; Obaje et al. 2020). The basin trends in the NW–SE direction, an NW extension of the Anambra Basin perpendicular to the main axis of the Benue Trough as shown in Fig. 1. Adeleye (1971) and Kogbe (1989) outlined three physiographic units that exist within the Basin. These are the flood plain of River Niger and its distributaries which flows ESE along the southern margin of the Basin, with a broad flood plain of about 20 km wide and series of elongated ponds that drains parallel to the river channel. Another physiographic unit is the discontinuous belt of mesas which covers about 10% of the Basin which

**Fig. 1** Geological map of Bida and environs, Nupe Basin, Nigeria



extends from 16 km east of Mokwa through the south to Baro, Lokoja, and southwest of Dekina area. The mesa-top is the northern dip of the Basin with an altitude between 150 m and 290 m above sea level along the Niger/Benue confluence area. However, there is an irregular dissection of the mesas by the distributaries of River Niger whose walls are always precipitous especially along the Niger-facing scarps. Along the mesa walls are intermediate breaks of slopes which indicates the presence of resistant beds. The third physiographic unit is the Plain which covers 70% of the Basin. It is flat-lying and gently rolling or flat-topped and sometimes breaks the unvarying landscape and is usually found along Mokwa-Bida and Bida-Zungeru roads. The plain lies between 120 and 360 m around Kontagora in the Northern part of the Basin, 120–240 m around Mokwa, 150–135 m at the Bida area, and 60–180 m along Lokoja to the south of the Basin.

The Nupe Basin is an intracratonic sedimentary basin with a northwest–southeast (NW–SE) trend (Adeleye 1974, Obaje 2009; Obaje et al. 2011a, b). The Nupe Basin is approximately 350 km long and varies in width from 75 to 150 km. It is roughly elliptical in ground plan and runs perpendicularly to the western margin of the NE–SW trending Benue Trough Complex. It is bounded to the northeast and southwest by the basement complex, to the southeast by the Anambra Basin, and the northwest by the Sokoto Basin as shown in Fig. 1. The origin of the basin has been linked to the sinistral offset that lies along the

northeastern–southwestern axis of the Benue Trough, which resulted in the reactivation of the mega-shears within the Precambrian basement (Benkhelil 1982; Burke and Dewey 1973). A major pattern of faulting was created which trend northeast–southwest and northwest–southeast to initiate the Nupe Basin, which was inclined perpendicular to the axis of the Benue Trough (Ajakaiye 1981; Benkhelil 1982). The basin was characterized as a northwestern extension of the adjoining southeast Anambra Basin since both were recorded as major depocenters at the third major transgressive cycle that took place during the late Cretaceous geologic time in southern Nigeria (Ojo 1984; Obaje 2009; Obaje et al. 2011a, b). Earlier studies divided the basin geographically into the northern and southern Bida Basin, probably due to the rapid facies changes across the basin (Obaje 2009; Obaje et al. 2011, b, 2020). The northern and southern Bida Basins comprise about 3.5-km thick Campanian to Maastrichtian continental to shallow marine sediments (Ladipo 1988; Obaje 2009; Obaje et al. 2011a, b). Gravity studies over the Bida Basin estimated that the sediments which include the Bida, Enagi and Batati Formation (ironstone) make up a maximum sedimentary thickness of about 3.5 km in the central axis (Ojo 1984). However, recent depth estimates of the residual magnetic field in different parts of the basin revealed an average sedimentary fill of about 3.4 km with a basement depth of up to 4.7 km estimated in the southern and central parts of the basin (Udensi and Osazua 2004). In

general, the depth to the basement in the basin is believed to decrease smoothly from the central parts to the flanks of the basin (Ladipo 1988; Ladipo et al. 1994; Braide1990; Obaje et al. 2011a, b, 2020). The southern Bida Basin comprises the basal Campanian Lokoja Formation, followed by the Maastrichtian Patti Formation and then the youngest Agbaja Formation which is also Maastrichtian in age (Ladipo 1988; Obaje 2009; Obaje et al. Obaje et al. 2011a, b). Their lateral stratigraphic equivalents in the northern Bida Basin consist of the basal Bida Formation.

The basin contains facies of post-orogenic molasse and thin unfolded sediments of marine origin which are lithostratigraphically correlated in successions to the cretaceous sediments of the Anambra and Sokoto Basins (Adeleye 1974). Ladipo (1988) and Ladipo et al. (1994), stated that the south-Atlantic Tethys Sea is believed to have transgressed through the Nupe Basin during the Campanian-Maastrichtian. Adeleye (1972) reclassified and upgraded the Nupe Sandstone to Nupe Group and further subdivided the Nupe Group into four distinct lithostratigraphic formations which include the Bida Sandstone, Sakpe Ironstone, Enagi Siltstone and Batati Ironstone Formations. The sedimentary deposits in the southern part of the Basin comprise the Campanian-Maastrichtian Basal Lokoja Formation which overlies the Precambrian basement non-conformably, while the Patti Formation is overlain by the Abaja Ironstone Formation (Adeleye and Dessauvage 1972), which is a lateral equivalent of the Enagi siltstone, Itakpe ironstone and Batati ironstone (sandstone), especially within the northwestern part of the basin. Integration of all these successions forms the lateral equivalents of the Campanian to Maastrichtian Mamu and Nsukka Formations as found in Anambra Basin. (Agyingi 1991). The deposits of the Lokoja Formation are made up of clay stones, sandstones, and conglomerates; which are alluvial fan deposits to the shallow marine environments (Akande et al. 2005). On the other hand, the Maastrichtian Patti Formation that overlies the Lokoja Formation consists of sandstones and shale-claystone deposited from a meandering river (Agyingi 1991).

## Materials and methods

The airborne magnetic data used in the present study are made up of four (4) high-resolution aeromagnetic (HRAM) maps obtained from the Nigeria Geological Survey Agency (NGSA 2011) and consists of aeromagnetic sheets covering Bida, Agbaje, Pategi, and Baro with sheet numbers 183, 184, 204 and 205. The high-resolution aeromagnetic data were acquired for the Nigerian Geology Survey Agency by Fugro between 2006 and 2009. The high-resolution aeromagnetic data were acquired with the use of a fixed-wing aircraft with 3 Scintrex CS-3 Cesium Vapor Magnetometers

mounted on the aircraft and recorded at an interval of 0.1 m with line spacing of 500 m in a series of NW–SE flight lines (perpendicular to the dominant regional geologic strike of the study), 2 km nominal tie-line spacing along the NE–SW direction with a terrain clearance of 80 m. The flight and tie lines trend with azimuths of  $135^{\circ}$  and  $45^{\circ}$  respectively. The geomagnetic gradient was removed from the data using the January 2005 IGRF model referenced to the World Geodetic System, 1984 ellipsoid. The aeromagnetic data were processed using several potential field softwares which includes Oasis Montaj 7.5 HJ version, the FOUR POT software, etc. The regional-residual separation technique using polynomial fitting was applied in this study. This is a purely analytical method in which matching of the regional by a polynomial surface of low order exposes the residual features as random errors. The regional gradients were removed by fitting a plane surface to the data by using multi-regression least-squares analysis to obtain the residual data. Upward continuation technique was carried out on the residual magnetic data to the height of 4 km to remove the short-wavelength components of the magnetic data. Figures 2 and 3 show the total magnetic field intensity (TMI) map and the regional map of the study area, respectively. The residual field map of the study area revealed high magnetic values with values ranging from about 0.4 to 82.4 nT (82.4 gammas) as shown in Fig. 4. Across the study area, magnetic highs were noticed majorly in the southern portion of the map as well as some parts of the northern section of the study area. The middle and northern sections of the study area associated with magnetic lows followed the location and trend of the Niger and Kaduna Rivers. These low magnetic areas are interpreted as the flood plains of the major drainages in the study area and are characterized by alluvial deposits.

## Centroid depth, geothermal gradient and heat flow estimation

Robust knowledge of the heat distribution within the earth's subsurface usually requires a detailed understanding of the centroid depth also known as the depth to the bottom of magnetic sources (DBMS) or Curie point depth (CPD). The CPD is a very important diagnostic parameter needed for heat flow estimates from spectral inversion of high-resolution aeromagnetic data. In this work, high-resolution aeromagnetic (HRAM) data were subdivided into sixteen (16) overlapping blocks with the depth to the top of magnetic sources (DTMS) and the depth to the bottom of magnetic sources (DBMS) estimated using spectral inversion techniques. Spectral analysis of the HRAM data was carried out using FOUR POT Potential Field Computer Software (Markku 2009). To compute the depth to the Curie point, the residual data of the study area were divided into sixteen spectral blocks using 110 km x 110 km spectral width. Curie

**Fig. 2** Total magnetic field intensity map of Bida and environs, Nupe Basin, in nano-teslas (nT)

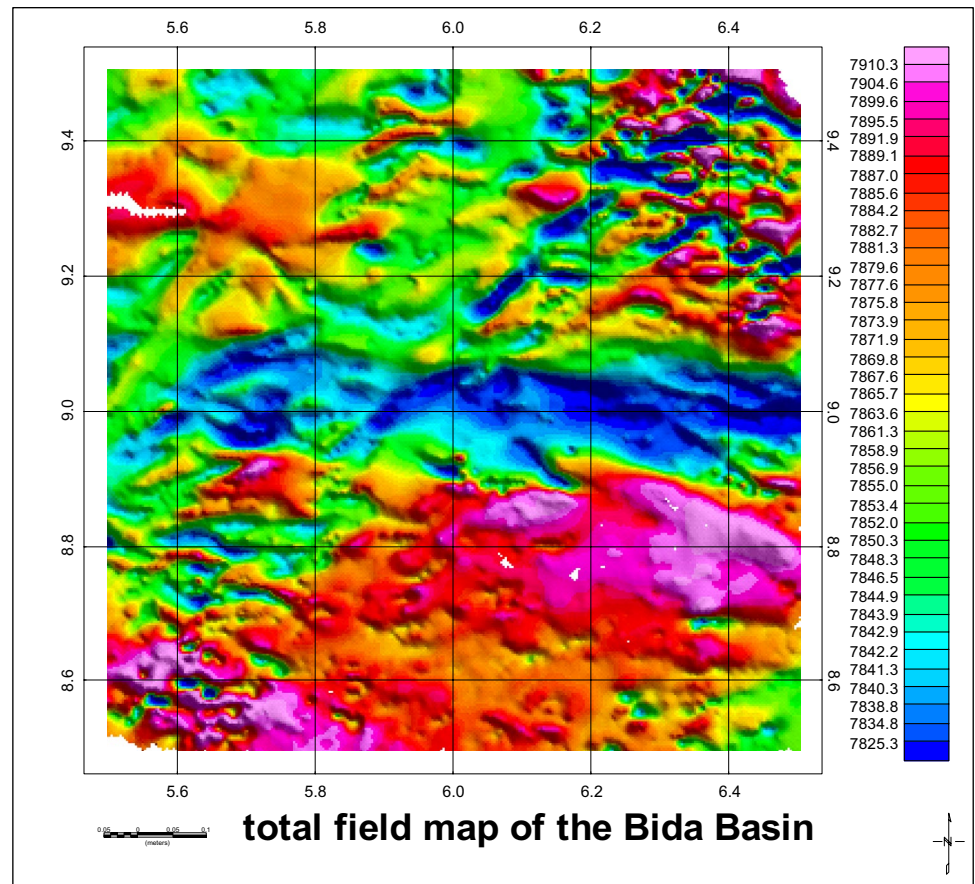


**Fig. 3** First degree regional field map of Bida and environs, Nupe Basin, in nano-teslas (nT)

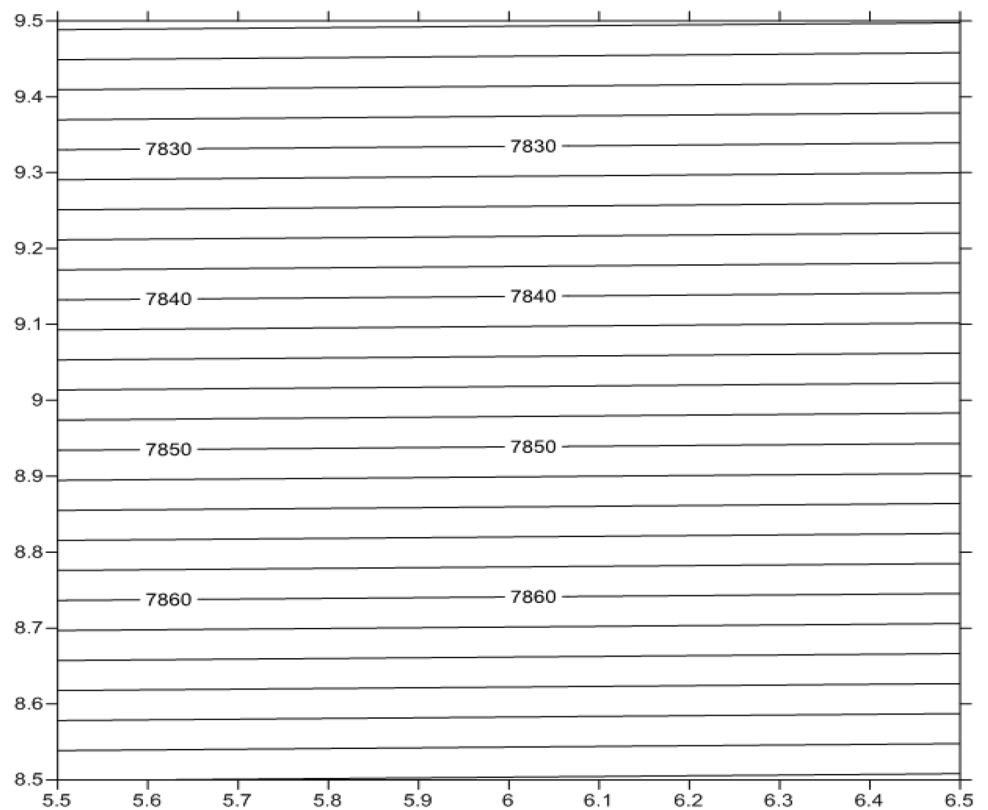
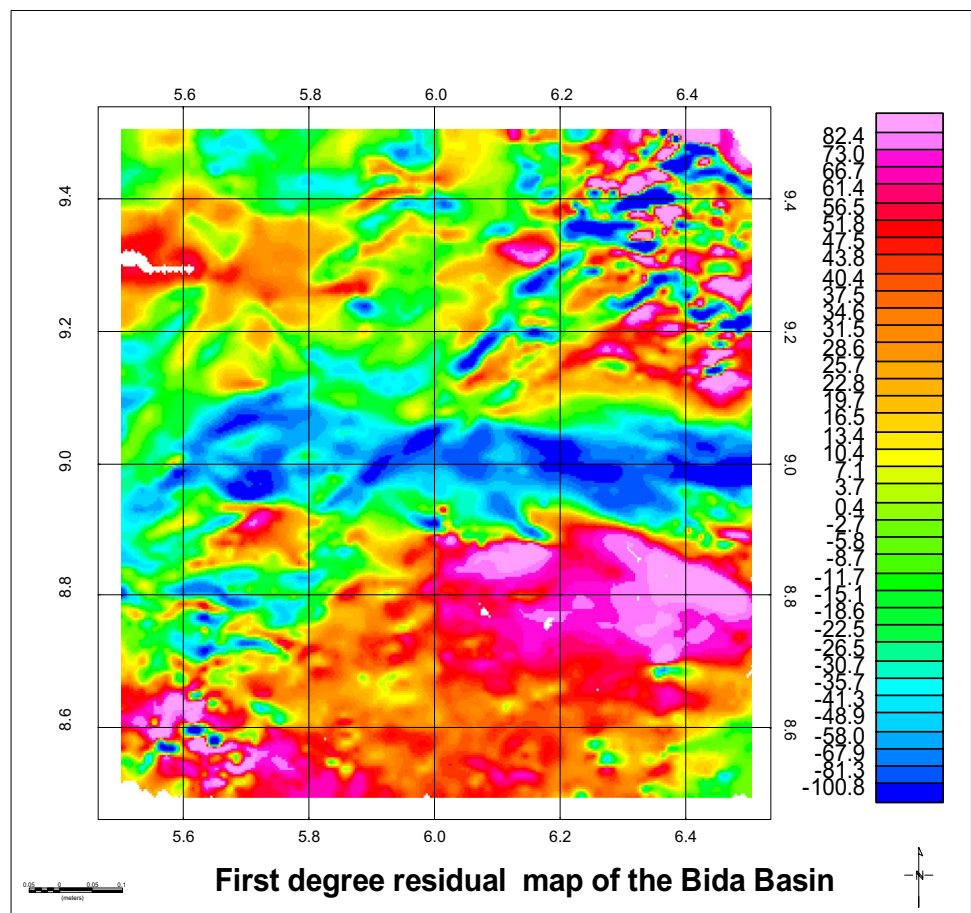


**Fig. 4** First degree residual field map of Bida and environs, Nupe Basin, in nano-teslas (nT)



point depth (CDP) estimation based on the spectral inversion of magnetic data has been widely used in the estimation of regional subsurface thermal regimes worldwide (Byerly and Stolt 1977; Tanaka et al. 1999). The technique is in line with the basic principles of the methods earlier adopted by Spector and Grant 1970. In the present study, the centroid depth ( $z_0$ ) was obtained according to the method adopted by Okubo et al. 1989; Okubo and Matsunaga 1994) using Eq. 1:

$$\ln \left[ \frac{p(k)^{\frac{1}{2}}}{k} \right] = A - kZ_0 \tag{1}$$

where  $P(k)$  represents the power density spectrum of the anomaly,  $k$  is the wavenumber,  $A$  is a constant, and  $z_0$  is the estimated depth to the centroid. The equation is valid in the range of  $k a \ll 1$ ,  $k D \ll 1$ , and  $\tan \theta \leq 1$ , where “ $a$ ” is half the horizontal thickness of the body, “ $D$ ” is half the vertical thickness of the body, and  $\theta$  is the dip of the body. Thus, a linear relationship exists between the wavenumber, the power density spectrum of the anomaly, and the estimated depth to the centroid,  $z_0$  (Eq. 1), suggesting that the centroid depth ( $Z_0$ ) can be obtained directly from the gradient of the spectrum (Okubo and Matsunaga 1994). However, Tanaka et al. (1999) stated that depth to the centroid of magnetic

sources may be calculated from the low wave-number portion of the wave-number scaled power spectrum as shown in Eq. 2:

$$\ln \left( \frac{p(k)^{\frac{1}{2}}}{k} \right) = B - |k|Z_t \tag{2}$$

where  $B$  is a constant and  $Z_0$  is the centroid depth of magnetic sources.

The depth to the top boundary  $Z_t$  and the depth to the centroid of the magnetic source  $s$  ( $Z_0$ ) were therefore estimated from the power spectrum of the magnetic anomalies, and were further utilized in estimating the basal depth to the magnetic sources  $Z_b$ . This was achieved through the application of Eq. (3) according to Okubo et al. (1985, 1989). The depth to the magnetic source (Curie point depth) was later derived using Eq. 3:

$$Z_b = 2Z_c - Z_t \tag{3}$$

where  $Z_t$  = depth to the top of the anomaly,  $Z_b$  = the basal depth, and  $Z_c$  = the centroid depth.

Kasidi and Nur (2012) suggested a one-dimensional heat conductive model which is based on the Fourier transform

law used for estimating geothermal gradient and heat flow as shown in Eq. 4:

$$q = \lambda \frac{dT}{dZ} \quad (4)$$

where  $q$  = the heat flow,  $\lambda$  = the coefficient of thermal conductivity, and  $\frac{dT}{dZ} = m$ . “ $m$ ” is the slope of the graph of change in temperature with depth. It is assumed to be a constant, since no loss or gain of heat (closed system) is usually recorded both above the crust and below the CPD. Tanaka et al. (1999) defined Curie temperature ( $\theta_c$ ) as shown in equation 5:

$$\theta = \left[ \frac{dT}{dZ} \right] Z_b \quad (5)$$

Therefore, substituting Eq. (5) into Eq. (4), we have:

$$q = \lambda \left[ \frac{\theta}{Z_b} \right] \quad (6)$$

Using a Curie point isotherm of 580 °C and thermal conductivity of 2.5 Wm<sup>-1</sup> °C<sup>-1</sup>, the heat flow can be calculated, from Eq. 6 (Tanaka et al. 1999; Nwankwo et al. 2009a, b; Elleta and Udensi 2012).  $Z_b$  = the basal depth,  $\theta$  = the standard Curie point isotherm of 580 °C,  $q$  = the heat flow, and  $\lambda$  = thermal conductivity which is given as 2.5 Wm<sup>-1</sup> C<sup>-1</sup> for igneous rocks.

## Results and discussion

The result of the Curie point depth, geothermal gradient, and heat flow was obtained from the spectral inversion technique of the high-resolution aeromagnetic data. The sample graphs of the logarithms of the power spectrum plots for some of the spectral blocks using the FOUR POT<sup>TM</sup> software are shown in Fig. 5. FOUR POT<sup>TM</sup> software is a program designed for the analysis of potential field data. To compute the depth to the centroid ( $Z_0$ ) and depth to the top of the magnetic anomaly ( $Z_t$ ), the residual magnetic data of the study area were divided into sixteen overlapping (16)

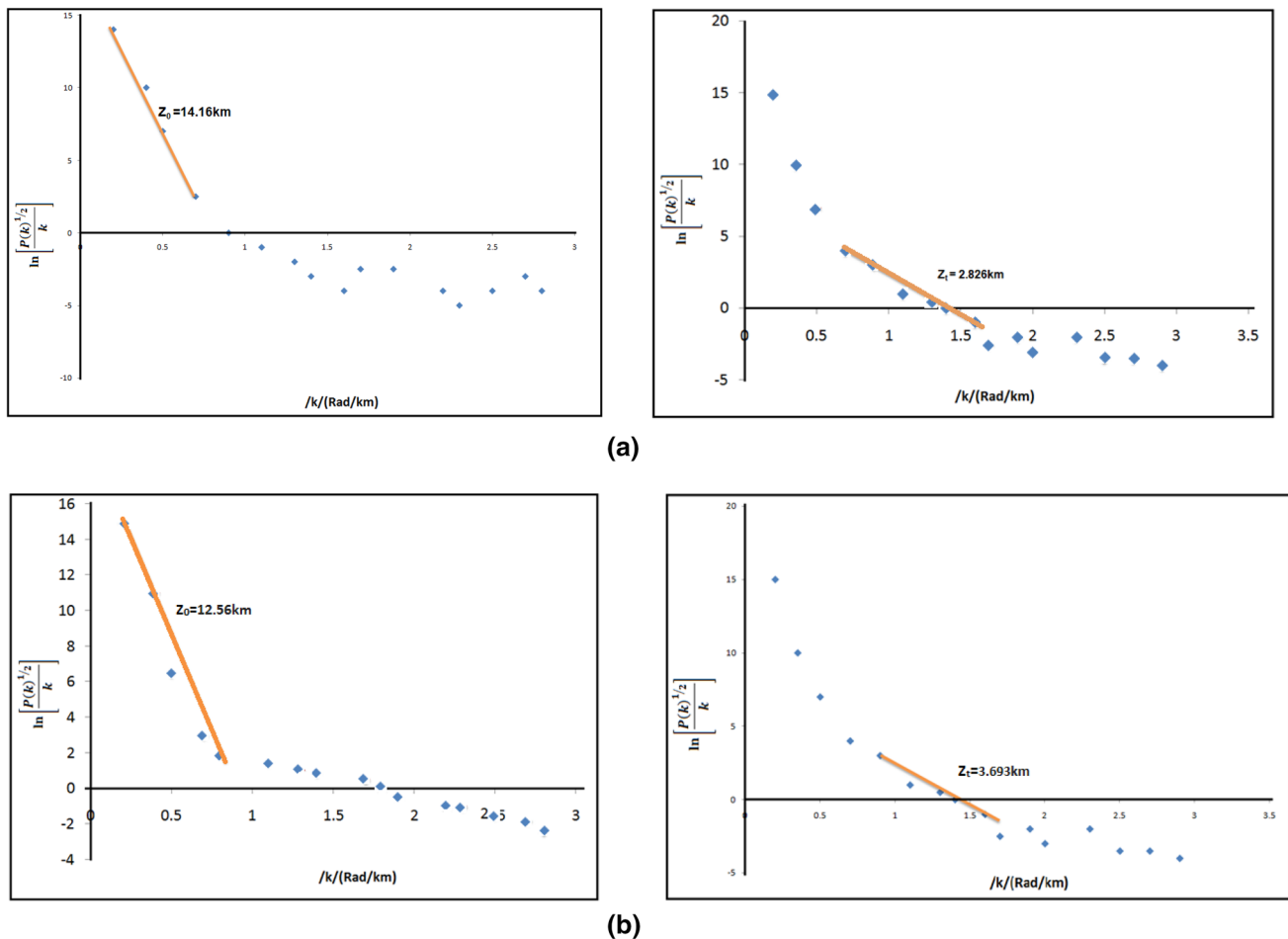


**Fig. 5** Representative spectral plots for some of the spectral blocks: **a**  $Z_0$  and  $Z_t$  for spectral block J. **b**  $Z_0$  and  $Z_t$  for spectral block N



spectral blocks of 110 km × 110 km windows. The results of the study revealed a two-layer depth model with the top layer representing the depth of magnetic sources ( $Z_t$ ), while the centroid depth of magnetic sources ( $Z_o$ ) is represented by the bottom layer. The depth to the centroid ( $Z_o$ ) was computed from the slope of the longest wavelength of the frequency-scaled power spectrum while the depth to the top of the magnetic anomaly ( $Z_t$ ) was also generated by computing the slope of the wavelength of the second-longest wavelength of the average power spectrum (Fig. 5).

The computed depths to the top boundary ( $Z_t$ ), the depth to the centroid ( $Z_o$ ) of the magnetic source, Curie point depth, geothermal gradient and heat flow are shown in Table 1. The depth to the top boundary ( $Z_t$ ) ranges from 2.184 km to 3.69 km with an average depth of 2.74 km, while the depth to the centroid ( $Z_o$ ) ranges from 12.26 km to 14.98 km with an average depth of 13.64 km. The estimated Curie point depths ( $Z_b$ ) from the study area ranges from 21.43 km as observed within spectral block N to 26.71 km within spectral block M, with an average value of 24.54 km. These values reflect the average local Curie point depth values observed beneath the subsurface rocks. The spatial map of the Curie point depth (Fig. 6) revealed that the highest CPD ( $Z_b$ ) values were noticed within the northern and western parts of the study area, while the lowest CPD values were recorded around the northeastern and northwestern sections of the study area.

The estimated geothermal gradient across the study ranged between 21.72 °C km<sup>-1</sup> for spectral block M and 27.07 °C

km<sup>-1</sup> for spectral block N around the Bida area, with an average of 24.39 °C km<sup>-1</sup>. Figure 7 shows the spatial map of the geothermal gradient across the study area which revealed a decrease in the geothermal gradient within the western, northern and southeastern parts of the study area. The map shows that areas around the NE and NW sections have the highest geothermal gradient values with values between 25.2 °C km<sup>-1</sup> and 27.2 °C km<sup>-1</sup>. It was revealed that the areas with high geothermal gradient corresponded to the areas with low Curie depth points and vice versa. Applying the thermal conductivity value of 2.5 Wm<sup>-1</sup>C<sup>-1</sup> as stated by Stacey (1977), to estimate the heat flow within the study area, the result (Table 1) revealed that the estimated heat flow ranges from 54.30 mWm<sup>-2</sup> at spectral block M to 67.67 mWm<sup>-2</sup> at spectral block N, with an average of 59.41 mWm<sup>-2</sup>. However, the highest heat flow was observed within the NE and NW portions of the study area, while the lowest heat flow values was observed at the central, western and NNW part of the study area (Fig. 8). Apart from the above-mentioned areas, other parts of the study area are associated with lower heat flow values as shown in Fig. 8.

The cross plot of the CPD versus the heat flow is shown in Fig. 9. The coefficient of determination ( $R^2$ ) for the plot revealed an  $R^2$  value of 0.997 indicating a strong correlation. The relationship between CPD and geothermal gradient, and between CPD and heat flow thus revealed an inverse relationship. The cross plot of Curie point depth (CPD) against the heat flow (HF) revealed an empirical relationship between

**Table 1** Geothermal Estimates of the study area calculated from spectral analysis

Spectral block	Longitude (°)		Latitude (°)		Spectral depth (km)		CPD (km)	Geothermal gradient (°Ckm <sup>-1</sup> )	Heat flow (m Wm <sup>-2</sup> )
	X <sub>1</sub>	X <sub>2</sub>	Y <sub>1</sub>	Y <sub>2</sub>	Z <sub>t</sub>	Z <sub>o</sub>	Z <sub>b</sub> = 2Z <sub>o</sub> - Z <sub>t</sub>	dT/dZ = θ/Z <sub>b</sub> θ = 580	q = K (dT/dZ) K = 2.5Wm <sup>-1</sup> C <sup>-1</sup>
A	5.50	5.75	8.5	8.75	2.526	13.62	24.714	23.468	58.671
B	5.75	6.00	8.5	8.75	2.764	14.01	25.256	22.965	57.412
C	5.75	6.00	8.75	9.00	2.485	13.97	25.455	22.785	56.963
D	5.50	5.75	8.75	9.00	2.574	13.98	25.386	22.847	57.118
E	6.0	6.25	8.5	8.75	2.383	13.52	24.657	23.523	58.807
F	6.25	6.50	8.5	8.75	2.282	13.75	25.218	22.999	57.499
G	6.25	6.50	8.75	9.00	2.184	13.82	25.456	22.784	56.961
H	6.0	6.25	8.75	9.00	2.245	13.29	24.335	23.834	59.585
I	5.50	5.75	9.00	9.25	2.946	14.67	26.394	21.975	54.937
J	5.75	6.00	9.00	9.25	2.826	14.16	25.494	22.750	56.876
K	5.75	6.00	9.25	9.50	2.865	14.75	26.635	21.776	54.440
L	5.50	5.75	9.25	9.50	2.972	12.35	21.728	26.694	66.734
M	6.0	6.25	9.00	9.25	3.254	14.98	26.706	21.718	54.295
N	6.25	6.50	9.00	9.25	3.693	12.56	21.427	27.069	67.672
O	6.25	6.50	9.25	9.50	2.894	12.26	21.626	26.820	67.049
P	6.0	6.25	9.25	9.50	2.943	12.53	22.117	26.224	65.560

**Fig. 6** Curie point depth map of the study area (Contour interval  $\sim 0.2$  km)

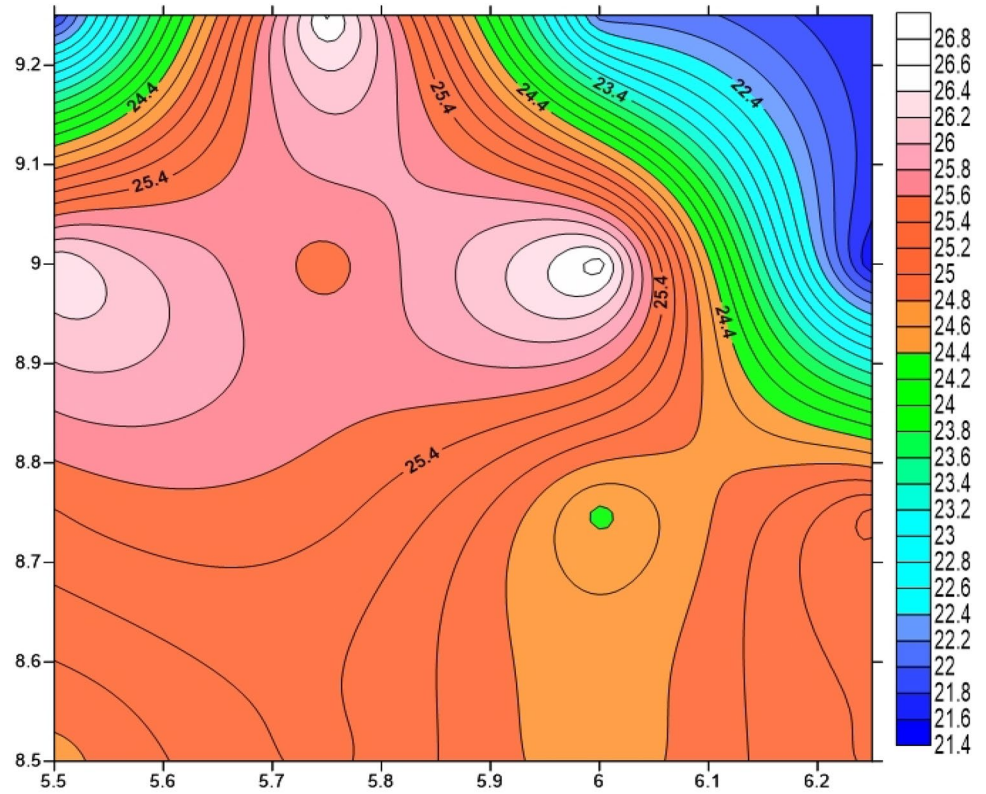


**Fig. 7** Geothermal gradient map of the study area (contour interval  $\sim 0.2$   $^{\circ}\text{C km}^{-1}$ )

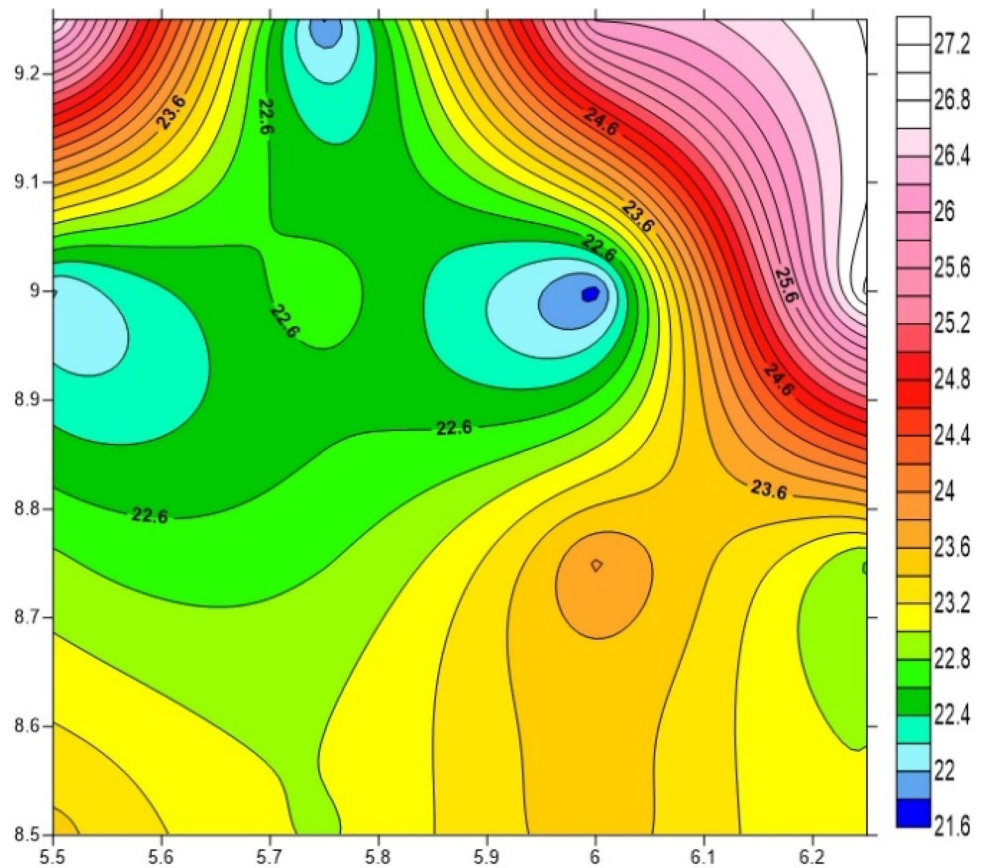


**Fig. 8** Heat flow map of the study area (contour interval  $\sim 0.5 \text{ Wm}^{-2}$ )

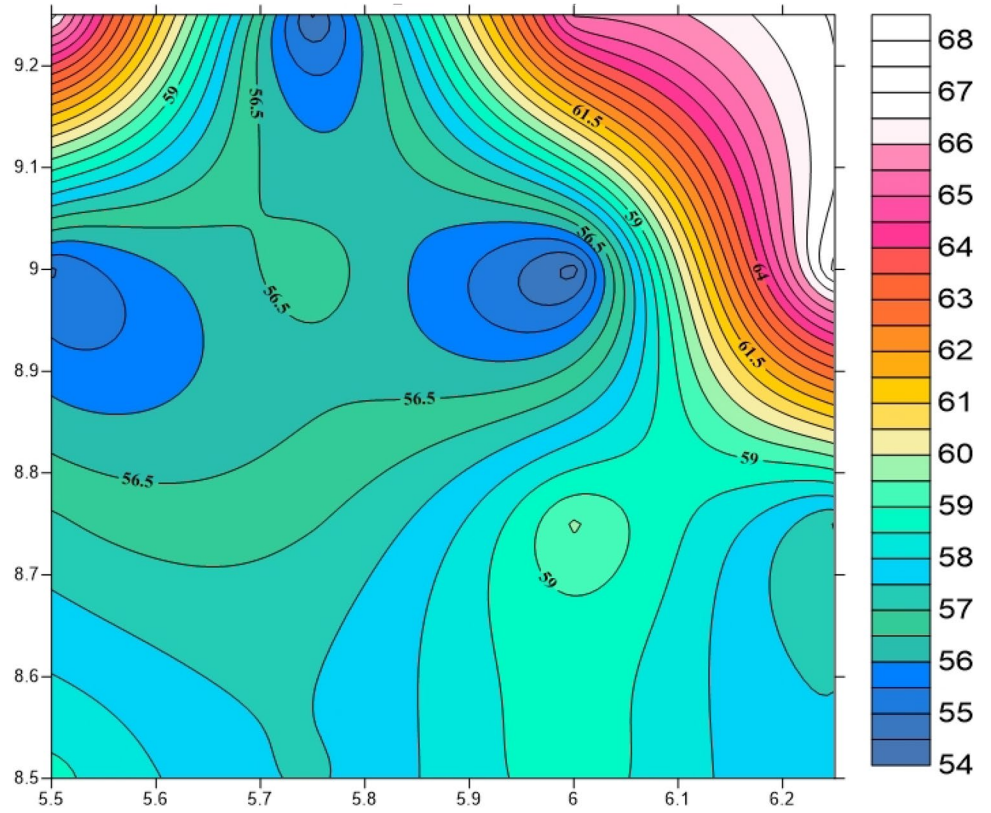
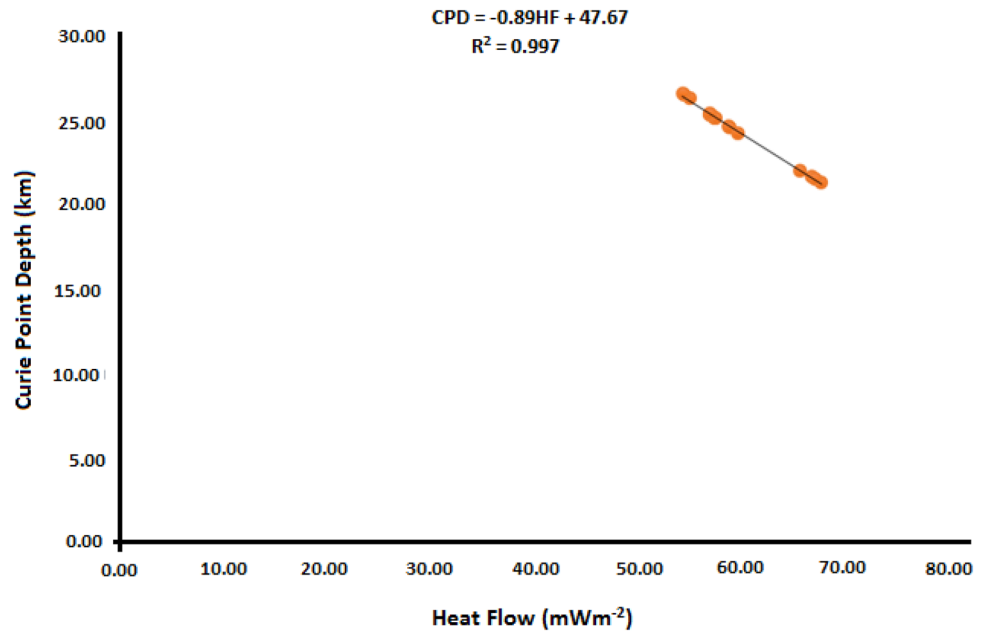


**Fig. 9** Cross plot of Curie point depth against heat flow



them as shown in Fig. 9. This relationship is represented by Eq. 7:

$$y = -0.389x + 47.67 \quad (7a)$$

where  $y$  = CPD (Curie point depth),  $x$  = HF (heat flow),  $-0.389$  is the slope of the graph, and  $47.67$  is the intercept. Therefore, Eq. 7a is then represented as Eq. 7b:

$$CPD = -0.389HF + 47.67 \quad (7b)$$

A similar empirical relationship was also established between the Curie point depth and the Geothermal Gradient as shown in Eq. 8:

$$CPD = -0.9733 \frac{dT}{dZ} + 47.688 \quad (8)$$

The high correlation coefficient obtained from these analytical plots which approaches ( $R^2 = 1$ ) therefore makes the relationship reliable.

Depths to the basement of deformed brittle and ductile rocks as well as their various modes of deformation are determined by their thermal structure (Nagata 1961). The presence of a geothermal play can be revealed through faulted structures (Feumoe and Ndougsa-Mbarga 2017), while the depth at which temperature rises to Curie point is assumed to be the bottom of magnetization of magnetic bodies within the crust. This temperature varies from one region to another as a result of geological complexity as well as the mineralogical composition of the underlying rocks. Therefore, it is imperative to know that areas of shallow Curie point depths are associated with regions with high geothermal potential, thinned crust and young volcanism. Since heat flow is an observable primary parameter used for exploring the geothermal energy of a field, areas with high heat flow and high geothermal gradient therefore generally correspond to igneous and metamorphic rich rocks. In continental regions, the normal thermal property is estimated at an average heat flow above  $60 \text{ m Wm}^{-2}$  and the range of  $80 \text{ mWm}^{-2}$ – $100 \text{ mWm}^{-2}$  for a considerable generation of geothermal energy (Jessop et al. 1976; Lawal et al. 2018). However, Jessop et al. (1976) stated that anomalous geothermal conditions arise when the thermal properties are above  $100 \text{ mWm}^{-2}$ . The spatial distribution of relatively high Curie Point Depth, geothermal gradient and heat flow of part of the Nupe Basin revealed a NE–SW and NW–SE trend and are believed to be associated with block faulting of the underlying basement (Nwankwo and Sunday 2017). These tectonic trends are associated with the paleo-structures (trans-oceanic fracture zones) including St Paul, Romanche, and Chain fracture systems with their major regional fault lines and echelon structures believed to have traversed the basin (Buser 1966; Ajakaiye et al. 1991; Nwankwo and Sunday 2017). These fault lines are believed to be landward

extensions of the trans-oceanic fracture systems which manifested as the West and Central Africa Rift Systems onshore. These lineaments and paleo-structures reflects areas of weakness and instability within the crust, and are associated with the Mid-Jurassic to Cretaceous opening of the Atlantic Ocean, whose reactivation took place during the early stages of continental rifting (Buser 1966; Ajakaiye et al. 1991; Nwankwo 2017). The observed trends of the thermal structure in the area is similar to the trends of trans-oceanic structures which tranversed the study area.

The results of the Curie point depth, geothermal gradient and heat flow of the study area range from 21.43 km to 26.71 km,  $21.72 \text{ }^\circ\text{C km}^{-1}$  to  $27.07 \text{ }^\circ\text{C km}^{-1}$ , and  $54.30 \text{ mWm}^{-2}$  to  $67.67 \text{ mWm}^{-2}$ , respectively. The Curie point depth was observed to have an inverse linear relationship with heat flow and geothermal gradient (Fig. 9). This plot shows a decrease in Curie point depth with an increase in heat flow as shown in Fig. 9. This agrees with the postulation that areas with significant geothermal energy are usually associated with anomalously high-temperature gradient and high heat flow, which is associated geothermally with a shallow Curie point depth (Kasidi and Nur 2013). Tectonically prone areas have been known to be associated with high geothermal gradient, high heat flow and low CPD. The result of the CPD, geothermal gradient and heat flow of the present study agrees with the work of Nwankwo et al. (Nwankwo et al. 2009a, b) which revealed that high Curie point depth, low geothermal gradient and low heat flow occur in areas underlain by sandstone which is in line with the area underlain by the Nupe sandstone as observed within the Wuya and Bida areas, whereas areas with low CPD, high geothermal gradient and high heat are underlain by porphyritic granite, schist/phyllites and mylonite as seen around Gbangba and Kutiwenji areas where the basement is closer to the surface. The thermal structure of the study area is best represented by CPD based on Okubo et al. 1989. Okubo et al. 1989 established that the nature, distribution and pattern of the Curie point depth is a very important index of the subsurface thermal trends because generally, the trend of CPD evaluated from the measured heat flow data of an area is usually similar to those estimated from spectral analysis of high-resolution aeromagnetic data of the area. In summary, the CPD pattern and trend usually reveals the thermal structural trend of any area (Okubo et al. 1989). The Curie point depth range of the area ( $\approx 26.64 - 21.4 = 5.2 \text{ km}$ ) is very small and thus implies that the study area falls within the same geological setting. With CPD values greater than 10 km, it, therefore, means that the study area is not a volcanic region and therefore does not have a very high potential geothermal reservoir. This is because Curie point depth is generally dependent on the prevailing geological conditions of the study area. Curie point depths are usually shallower than 10 km for volcanic and geothermal fields,

between 15 and 25 km for island arcs and ridges, and deeper than 20 km in plains, plateaus and trenches (Okubo et al. 1989; Jessop et al. 1976; Ladipo 1988). Since the mean heat flow regime in thermally non-active continental regions is usually around 60 mW/m<sup>2</sup>, therefore areas with heat flow values within or higher than the heat flow range of 80–100 mW/m<sup>2</sup> indicate anomalous geothermal conditions (Jessop et al. 1976). Therefore, continental areas with heat flow values greater than 60 mW/m<sup>2</sup> are usually recommended for further geothermal exploration. Geothermal gradients in such areas therefore may provide a potential source(s) of geothermal energy, with associated Curie temperatures greater than 24 °C most often reached at depths of less than 2 km in such areas.

## Conclusion

The Curie point depth, geothermal gradient and heat flow values were estimated from the spectral inversion of the HRAM data of Bida and environs, Nupe Basin, Nigeria. Top depths to magnetic sources across the area were in the range of 2.184 km–3.69 km with an average depth of 2.74 km, whereas the centroid depths range from 12.26 km to 14.98 km with an average depth of 13.64 km. The geothermal gradient values were estimated to be in the range of 17.98–23.95 °C km<sup>-1</sup> with an average value of 21.62 °C km<sup>-1</sup>. Finally, the heat flow values range from 54.30 mWm<sup>-2</sup> to 67.67 mWm<sup>-2</sup> with an average of 59.41 mWm<sup>-2</sup>. Generally, CPD values greater than 10 km imply that the area is not a volcanic area or a potential geothermal reservoir. Therefore, since the study area is a thermally non-active continental area with heat flow values greater than 60 mW/m<sup>2</sup> in some sections, it is therefore that the area should be subjected to further geothermal exploration.

**Acknowledgements** The authors acknowledge with thanks the support of the Management of the Federal University of Technology, Owerri, Nigeria, during the period of this research work. The Management of the Nigerian Geological Survey Agency (NGSA) is deeply appreciated for the release of the high-resolution aeromagnetic (HRAM) data and the geoscientific softwares used in this study.

## Compliance with ethical standards

**Conflict of interest** The authors have declared that no conflicting interest exists.

## References

Abd-El-Nabi, S. H. (2012). Curie point depth beneath the Barramiya-Red Sea coast area estimated from aeromagnetic spectral analysis. *Journal of Asian Earth Sciences*, 43, 254–266.

- Abraham, E. M., Lawal, K. M., Ekwe, A. C., Alile, O., Murana, K. A., & Lawal, A. A. (2014). Spectral analysis of aeromagnetic data for geothermal energy investigation of Ikogosi Warm Spring–Ekiti State, southwestern Nigeria. *Geothermal Energy*, 2, 1–21.
- Abraham, E. M., Obande, E. G., Chukwu, M., Chukwu, C. G., & Onwe, M. R. (2015). Estimating Depth to the bottom of Magnetic Sources at Wikki Warm Spring Region, Northern Nigeria, using Fractal Distribution of Sources Approach. *Turkish Journal of Earth Science*, 24, 1–19.
- Abraham, E., Tumoh, O., Chukwu, C., & Rock, O. (2018). Geothermal Energy Reconnaissance of Southeastern Nigeria from Analysis of Aeromagnetic and Gravity Data. *Pure and Applied Geophysics, Springer Nature Switzerland AG.* <https://doi.org/10.1007/s00024-018-2028-1>.
- Adeleye, D. R. (1971). *Stratigraphy and Sedimentation of the Upper Cretaceous Strata around Bida, Nigeria* (p 297). Thesis, Univ. of Ibadan.
- Adeleye, D. R. (1974). Sedimentology of the fluvial Bida Sandstones (Cretaceous) Nigeria. *Sedimentary Geology*, 12, 1–24.
- Adeleye, D. R., & Dessauvage, T. F. J. (1972). Stratigraphy of the Embayment near Bida, Nigeria. In T. F. J. Dessauvage & A. J. Whiteman (Eds.), *African Geology* (pp. 181–185). Ibadan: University of Ibadan Press.
- Agyingi, C. (1991). *Geology of upper Cretaceous rocks in the eastern Bida Basin, Central Nigeria* (p. 501). Unpublished Ph. D Thesis, University of Ibadan
- Ajakaiye, D. E. (1981). Geophysical investigations in the Benue trough—a review. *Earth Evolution Sciences*, 2, 110–125.
- Ajakaiye, D. E., Hall, D. H., Ashiekaa, J. A., & Udensi, E. E. (1991). Magnetic anomalies in the Nigerian continental mass based on aeromagnetic surveys. *Tectonophysics*, 192, 211–230.
- Akande, S. O., Ojo, O. J., & Ladipo, K. (2005). *Upper Cretaceous sequences in the southern Bida Basin* (p. 60p). Nigeria; A Field Guidebook: Mosuro Publishers, Ibadan.
- Badalyan, M. (2000). Geothermal features of Armenia: A country update. In *Proceedings World Geothermal Congress* (pp. 71–76). Kyushu-Tohoku, Japan.
- Banerjee, B., Subba Rao, P. B. V., Gautam Gupta, E. J., & Singh, B. P. (1998). Results from a magnetic survey and geomagnetic depth sounding in the post-eruption phase of the Barren Island volcano. *Earth Planets Space*, 50, 327–338. <https://doi.org/10.1186/BF03352119>.
- Bansal, A. R., Anand, S. P., Rajaram, M., Rao, V. K., & Dimri, V. P. (2013). Depth to the bottom of magnetic sources (DBMS) from aeromagnetic data of Central India using a modified centroid method for fractal distribution of sources. *Tectonophysics*, 603, 155–161.
- Bansal, A. R., Gabriel, G., Dimri, V. P., & Krawczyk, C. M. (2011). Estimation of depth to the bottom of magnetic sources by a modified centroid method for fractal distribution of sources: An application to aeromagnetic data in Germany. *Geophysics*, 76(L3), L11–L22. <https://doi.org/10.1190/1.3560017>.
- Bello, R., Ofoha, C. C., & Wehiuzo, N. (2017). Geothermal Gradient, Curie Point Depth and Heat Flow Determination of Some Parts of Lower Benue Trough and Anambra Basin, Nigeria, Using High-Resolution Aeromagnetic Data. *Physical Science International Journal*, 15(2), 1–11.
- Benkhelil, J. (1982). Benue Trough and Benue Chain. *Geological Magazine*, 119(2), 155–168. <https://doi.org/10.1017/S001675680002584X>.
- Bertani, R. (2010). Geothermal power production in the world 2005–2010 update report. In *Proceedings of WGC*(8:41). Bali, Indonesia: 2010.
- Bhattacharyya, B. K. (1966). Continuous spectrum of the total Magnetic field Anomaly due to Rectangular Prismatic Body. *Geophysics*, 31(1), 97–121.

- Bhattacharyya, B. K., & Leu, L. K. (1975). Spectral analysis of gravity and magnetic anomalies due to two-dimensional structures. *Geophysics*, *40*, 993–1013.
- Blakely, R. J. (1988). Curie temperature isotherm analysis and tectonic implications of aeromagnetic data from Nevada. *Journal of Geophysical Research*, *93*, 817–832.
- Blakely, R. J., & Hassanzadeh, S. (1981). Estimation of depth to the magnetic source using maximum entropy power spectra with application to the Peru-Chile trench. *Geological Society of America Memoir*, *154*, 667–681.
- Braide, S. P. (1990). *Petroleum geology of the Southern Bida Basin, Nigeria*. United States: N. p Journal Volume: 74:5; Conference: Annual convention and exposition of the American Association of Petroleum Geologists, San Francisco, CA (USA), 3–6 Jun 1990; Journal ID: ISSN 0149-1423.
- Burke, K., & Dewey, J. F. (1973). Plume-generated triple junctions: key indicators in applying plate tectonics to old rocks. *Journal of Geology*, *81*, 406–433.
- Buser, H. (1966). *Paleostructures of Nigeria and adjacent countries*. Stuttgart: Schweizerbart'sche Verlagsbuchhandlung.
- Byerly, P. E., & Stolt, R. H. (1977). An attempt to define the Curie point isotherm in northern and central Arizona. *Geophysics*, *42*, 1394–1400.
- Connard, G., Couch, R., & Gemperle, M. (1983). Analysis of aeromagnetic measurements from the Cascade Range in central Oregon. *Geophysics*, *48*, 376–390.
- Dolmaz, M. N., Ustaomer, T., Hisarli, Z. M., & Orbay, N. (2005). Curie Point Depth variations to infer the thermal structure of the crust at the African-Eurasian convergence zone, SW Turkey. *Earth Planets Space*, *57*, 373–383.
- Elleta, B. E., & Udensi, E. E. (2012). Investigation of the Curie point Isotherm from the Magnetic Fields of Eastern Sector of Central Nigeria. *Geosciences*, *2*(4), 101–106.
- Ewa, K., & Kryrowska, S. (2010). Geothermal exploration in Nigeria. *Proceedings World Geothermal Congress Zaria, Nigeria*, *3*, 1–59.
- Faulds, J. E., Coolbaugh, M., Bouchot, V., Moeck, I., & Oguz, K. (2010). Characterizing structural controls of geothermal reservoirs in the basin and range, USA, and western Turkey: developing successful exploration strategies in extended terrains. In: *Proceedings of the WGC Bali, Indonesia* (p. 11). April 25–30, 2010.
- Feumoe, A. N. S., & Ndougsa-Mbarga, T. (2017). Curie Point Depth Variations Derived from Aeromagnetic Data and the Thermal Structure of the Crust at the Zone of Continental Collision (South-East Cameroon). *Geophysica*, *52*(1), 31–45.
- Heicken, G. (1982). Geology of geothermal systems. In L. M. Edwards, G. V. Chilingar, H. H. Rieke, & W. H. Fertl (Eds.), *Handbook of Geothermal Energy* (pp. 177–217). Houston: Gulf Publishing Company.
- Hisarli, Z.M. (1996). *Determination of Curie Point Depths in Western Anatolia and Related with the Geothermal Areas*, Ph.D. Thesis. Istanbul University, Turkey (Unpubl.).
- Hsieh, H. H., Chen, C. H., Lin, P. Y., & Yen, H. Y. (2014). Curie Point Depth from Spectral Analysis of Magnetic data in Taiwan. *Journal of Asian Earth Sciences*, *90*, 26–33.
- IPCC. (1990). Climate Change. In J. T. Houghton, G. J. Jenkins, & J. J. Ephraums (Eds.), *The Intergovernmental Panel on Climate Change Scientific Assessment* (p. 365). Cambridge: Cambridge University Press.
- IPCC. (2014). Climate Change 2014: Impacts, Adaptation, and Vulnerability. In V. R. Barros, C. B. Field, D. J. Dokken, M. D. Mastrandrea, K. J. Mach, T. E. Bilir, M. Chatterjee, K. L. Ebi, Y. O. Estrada, R. C. Genova, B. Girma, E. S. Kissel, A. N. Levy, S. MacCracken, P. R. Mastrandrea, & L. L. White (Eds.), *Part B: Regional Aspects: Contribution of Working Group II to the Fifth Assessment Report of the Intergovernmental Panel on Climate Change*. Cambridge: Cambridge University Press.
- Jessop, A. M., Habart, M. A., & Sclater, J. G. (1976). The world heat data collection 1976, Geothermal Services of Canada. *Geotherm. Ser.*, *50*, 251–266.
- Kasidi, S., & Nur, A. (2012). Curie depth isotherm deduced from spectral analysis of Magnetic data over Sarti and environs of North-Eastern Nigeria. *International Journal of Earth Science and Engineering*, *5*(1), 1284–1290.
- Kasidi, S., & Nur, A. (2013). Estimation of Curie Point Depth, Heat Flow, and Geothermal Gradient Inferred from Aeromagnetic Data over Jalingo and Environs North-Eastern Nigeria. *International Journal of Science Emerging Tech*, *6*(6), 294–301.
- Khojamli, A., Ardejani, F. D., Moradzadeh, A., Kalate, A. N., Kahoo, A. R., & Porkhial, S. (2016). Estimation of Curie point depths and heat flow from Ardebil province, Iran, using aeromagnetic data. *Arabian Journal of Geosciences*, *9*, 383.
- Kogbe C.A. (1989). *Geology of Nigeria*, 2nd revised edition, Rock View (Nigeria) Limited, 1234 Zaramaganda, km 8 Yakubu Gowon way Jos.
- Ladipo, K. O. (1988). Paleogeography Sedimentation and Tectonics of the upper Cretacemes Anambra Basin, South-eastern Nigeria. *Journal of African Earth Sciences*, *7*, 865–871.
- Ladipo, K. O., Akande, S. O., & Mucke, A. (1994). The genesis of Ironstones from the Mid-Niger sedimentary basin: Evidence from sedimentological, Ore microscopic, and geochemical studies. *Journal of Mining and Geology*, *30*, 161–168.
- Lawal, T. O., & Nwankwo, L. I. (2017). Evaluation of the depth to the bottom of magnetic sources and heat flow from high resolution aeromagnetic (HRAM) data of part of Nigeria sector of Chad Basin. *Arabian Journal of Geosciences*, *10*, 378. <https://doi.org/10.1007/s12517-017-3154-2>.
- Lawal, T. O., Nwankwo, L. I., Iwa, A. A., Sunday, J. A., & Orosun, M. M. (2018). Geothermal Energy Potential of the Chad Basin, North-Eastern Nigeria. *J. Appl. Sci. Environ. Manage.*, *22*(11), 1817–1824.
- Leary, P., Malin, P., Shalev, E., et al. (2013). *Log normally Distributed K/Th/U Concentrations—Evidence for Geo-Critical Fracture Flow* (pp. 1–14). Los Azufres Geothermal Field, MX. GRC Trans.
- Markku, P., (2009). *Fourier transform based processing of 2D potential field data Version 1.0a (software)*. Division of Geophysics, Department of geosci FIN- 90014, University of Oulu, Finland.
- Moeck, I. S. (2014). Catalog of geothermal play types based on geologic controls. *Renewable and Sustainable Energy Reviews*, *37*, 867–882.
- Muffler, L. J. P. (1976). Tectonic and hydrologic control of the nature and distribution of geothermal resources. In *Proceedings of the 2nd U.N. Symposium of the development and use of geothermal resources* (pp. 499–507).
- Nagata, T. (1961). *Rock Magnetism* (p. 350). Tokyo: Maruzen Company Ltd.
- NGSA. (2011). *Nigerian Geological Survey Agency Nationwide Aeromagnetic Report* (p. 560)
- Nwankwo, C. N., Ekine, A. S., & Nwosu, L. I. (2009a). Estimation of the Heat Flow Variation in the Chad, Basin. *Nigeria. J. Appl. Sci. Environ. Manage.*, *13*, 73–80.
- Nwankwo, L. I., Olasehinde, P. I., & Akoshile, C. O. (2009b). An attempt to estimate the Curie Point Isotherm depth in the Nupe Basin, west Central Nigeria. *Global Journal of Pure and Applied Sciences*, *15*(3), 427–433.
- Nwankwo, L. I., Olasehinde, P. I., & Akoshile, C. O. (2011). Heat flow anomalies from the spectral analysis of Airborne Magnetic data of Nupe Basin, Nigeria. *Asian Journal of Earth Sciences*, *1*, 1–6.
- Nwankwo, L. I., & Sunday, A. J. (2017). Regional estimation of Curie-point depths and succeeding geothermal parameters from recently

- acquired high-resolution aeromagnetic data of the entire Bida Basin, north-central Nigeria. *Geoth. Energy. Sci.*, 5, 1–9.
- Obaje, N.G. (2009). *Geology and Mineral Resources of Nigeria*. Lecture Notes in Earth Sciences (p. 120). Berlin: Springer.
- Obaje, N. G., Bomai, A., Moses, S. D., Ali, M., Aweda, A., Habu, S. J., et al. (2020). Updates on the Geology and Potential Petroleum System of the Bida Basin in Central Nigeria. *Petroleum Science and Engineering*, 4(1), 23–33. <https://doi.org/10.11648/j.pse.20200401.13>.
- Obaje, N. G., Moumouni, A., Goki, N. G., & Chaanda, M. S. (2011a). Stratigraphy, Paleogeography and Hydrocarbon Resource Potentials of the Bida Basin in North-Central Nigeria. *Journal of Mining and Geology*, 47(2), 97–114.
- Obaje, N., Musa, M., Odoma, A., & Hamza, H. (2011b). The Bida Basin in North-central Nigeria: sedimentology and petroleum geology. *Journal of Petroleum and Gas Exploration Research*, 1(1), 1–13.
- Obande, G. E., Lawal, K. M., & Ahmed, L. A. (2014). Spectral analysis of aeromagnetic data for the geothermal investigation of Wikki Warm Spring, north-east Nigeria. *Geothermics*, 50, 85–90.
- Ojo, S. B. (1984). Middle Niger Basin revisited: magnetic constraints on gravity interpretations. In *Abstract, 20th Conference of the Nigeria Mining and Geosciences Society, Nsukka* (pp. 52–53).
- Okubo, Y., Graft, R. J., Hansen, R. O., Ogawa, K., & Tsu, H. (1985). Curie point depths of the Island of Kyushu and surrounding areas. *Japan. Geophysics*, 53(3), 481–494.
- Okubo, Y., & Matsunaga, T. (1994). Curie point depth in northeast Japan and its correlation with regional thermal structure and seismicity. *Journal of Geophysical Research: Solid Earth*, 99, 22363–22371.
- Okubo, Y., Tsu, H., & Ogawa, K. (1989). Estimation of Curie Point Temperature and Geothermal Structure of Island Areas of Japan. *Tectonophysics*, 159, 279–290.
- Opara, A. I., Odumosu, G. E., Akaolisa, C. Z., Onyekuru, S. O., Emberga, T. T., & Onu, N. N. (2018). Basement Depth Re-Evaluation and Structural Kinematic Analysis of Part of the Middle Benue Trough using High Resolution Aeromagnetic Data. *FUTO Journal Series (FUTOJNLS)*, 4(1), 409–436.
- Saleh, S., Salk, M., & Pamukcu, O. (2013). Estimating Curie point depth and heat flow map for northern Red Sea rift of Egypt and its surroundings, from aeromagnetic data. *Pure and Applied Geophysics*, 170, 863–885.
- Şalk, M., Pamukçu, O., & Kaftan, İ. (2005). Determination of the Curie point depth and heat flow from Magsat data of western Anatolia. *J. Balkan Geophys. Soc.*, 8, 149–160.
- Sayed, E., Selim, I., & Aboud, E. (2013). Application of spectral analysis technique on ground magnetic data to calculate the Curie depth point of the eastern shore of the Gulf of Suez. *Egypt. Arabian Journal of Geosciences*, 7, 1749–1762.
- Shuey, R. T., Schellinger, D. K., Tripp, A. C., & Alley, L. B. (1977). Curie depth determination from aeromagnetic spectra. *Geophys. J. the Roy. Astr. Soc.*, 50, 75–101.
- Smith, R. B., Shuey, R. T., Freidline, R. O., Otis, R. M., & Alley, L. B. (1974). Yellowstone Hot Spot: New magnetic and seismic evidence. *Geology*, 2, 451–455.
- Smith, R. B., Shuey, R. T., Pelton, J. R., & Bailey, J. P. (1977). Yellowstone hotspot: Contemporary tectonics and crustal properties from the earthquake and aeromagnetic data. *Journal Geophysical Research*, 82, 3665–3676.
- Soltani, M., Kashkooli, F. M., Dehghani-Sanij, A. R., Nokhosteen, A., Ahmadi-Joughi, A., Gharali, K., et al. (2019). 2019. *A Comprehensive Review of Geothermal Energy Evolution and Development*, *International Journal of Green Energy*, 16(13), 971–1009.
- Spector, A., & Grant, F. S. (1970). Statistical models for interpreting aeromagnetic data. *Geophysics*, 35, 293–302.
- Stacey, F. D. (1977). *Physics of the Earth* (2nd ed.). New York: John Wiley & Sons.
- Stampolidis, A., Kane, I., Tsokas, G. N., & Tsourlo, P. (2005). Curie point depths of Albania inferred from ground total field magnetic data. *Surveys In Geophysics*, 26, 461–480.
- Stampolidis, A., & Tsokas, G. N. (2002). Curie point depths of Macedonia and Thrace, N. Greece. *Pure and Applied Geophysics*, 159, 2659–2671.
- Tanaka, A., Okubo, Y., & Matsubayashi, O. (1999). Curie point depth based on spectrum analysis of the magnetic anomaly data in East and Southeast Asia. *Tectonophysics*, 306, 461–470.
- Udensi, E. E., & Osazua, I. B. (2004). The spectral determination of depths to magnetic rocks under the Nupe Basin, Nigeria. *Nigerian Associations of Petroleum explorationists (NAPE), Bull.*, 17, 22–27.
- Vacquier, V., & Affleck, J. (1941). A Computation of average depth the bottom of the Earth's magnetic crust, based on a statistical study of local magnetic anomalies. *Trans. Amer. Geophys. Union*, 22, 446–450.